ELSEVIER

International Journal of Mass Spectrometry 216 (2002) 257–268

International Journal of Mass Spectrometry

www.elsevier.com/locate/ijms

Effects of drift-gas polarizability on glycine peptides in ion mobility spectrometry

Luther W. Beegle [a], Isik Kanik [a,*], Laura Matz [b], Herbert H. Hill, Jr. [b]

[a] *Jet Propulsion Laboratory, California Institute of Technology, Pasadena, CA 91109, USA*
[b] *Department of Chemistry, Washington State University, Pullman, WA 99164-4630, USA*

Received 9 March 2001; accepted 5 March 2002

Abstract

This investigation is a continuation of our previous work on the feasibility of utilizing ultra-high resolution electrospray ionization/ion mobility spectrometry (ESI/IMS) for in situ analysis of biomolecular compounds. The compounds we studied, in this investigation, were glycine, the smallest amino acid and four of its oligomers, namely triglycine, tetraglycine, pentaglycine, and hexaglycine. Experimental effects of drift-gas polarizability on target ions in IMS were explored by utilizing four different drift-gases with differing polarizability values (He, Ar, N_2, and CO_2). The gas-phase ion radii for all five compounds were calculated from the reduced ion mobilities, K_0^m, and the effective drift-gas radii employing a simple hard-sphere model. When ion radii were plotted against the polarizabilities of the drift-gases, linear plots with different slopes were produced. This empirical observation indicated that the polarizing of drift-gas can change the calculated ion radii in a linear fashion over a limited range of polarizability values and does not affect all ions equally. This effect can be exploited in order to alter the separation factors between different ions since all ions that yield different slopes can, theoretically, be separated with IMS using different drift-gases. We demonstrated that the separation factor (α) is highly dependent on the drift-gas. The maximum separability and, hence, unique identification of target ions was achieved when He and CO_2 were used. (Int J Mass Spectrom 216 (2002) 257–268) © 2002 Published by Elsevier Science B.V.

Keywords: Ion mobility; Drift tubes; Polarization

1. Introduction

The developing field of astrobiology tries to answer the question of whether life once existed or now exists elsewhere in the solar system. Organic analysis of surface material will be of pivotal importance as the question is further elucidated. Biosignatures of past life may still exist today both on Mars and Europa in some protected subsurface environments such as beneath the surface of Martian polar ice caps [1] or inside the icy surface of Europa [2]. An efficient, fast and accurate in situ chemical analysis of melt water, which might carry biomarkers of past (or present) life, should be one of the major science goals of future Mars and Europan landers. State-of-the-art detection techniques suitable for in situ detection of large organic molecules of biological importance, that would also be highly selective and sensitive (parts per billion) to specific organic compounds, will play a major role in these endeavors. One of the main components of the science payload in future missions will most certainly be an analytical separation device which could

* Corresponding author. E-mail: ikanik@pop.jpl.nasa.gov

1387-3806/02/$ – see front matter
PII S1387-3806(02)00626-7

identify extant or extinct signatures of life (i.e., amino acids, peptides, proteins, etc.) which may be present there.

This is the second in a planned series of papers [3] exploring the feasibility of utilizing an electrospray ionization/ion mobility spectrometer (ESI/IMS) technique as a stand alone analytical separation tool in analyzing biomolecular compounds. Since amino acids represent one of the most basic chemical signatures of life, we utilized 19 amino acids common to terrestrial biology to conduct the first part of our laboratory feasibility studies using the high-resolution ESI/IMS technique [3]. In the present investigation, we targeted four peptides consisting entirely of the amino acid, glycine. We report the ion mobility constants of glycine along with four peptide compounds (triglycine, tetraglycine, pentaglycine, and hexaglycine) in four different drift-gases (He, Ar, N_2, and CO_2). We also report the effects of different drift-gases in IMS on the calculated ion radii of the peptide compounds. The gas-phase ion radii were calculated and plotted against the polarizability of each drift-gas used, producing linear plots. The slope of these lines provided information on the magnitude of the ion's mobility as a function of polarizability whereas the intercept provided a theoretical gas-phase radius of the ion in an unpolarized medium.

IMS has many features that make it attractive as an analytical separation device. IMS is simple, fast, rugged, highly selective, and very sensitive to a wide range of compounds. IMS is a sensitive field detection technique which can readily measure ion currents below 10^{-12} A [4]. IMS has found wide use for detection of volatile chemical compounds such as explosives, narcotics, and chemical warfare agents [5]. Due to the recent developments in the ESI technique, investigators have been able to carry out analysis of nonvolatile chemicals directly from liquid phase samples utilizing IMS in tandem with ESI [6]. The development of ESI/IMS greatly expanded the range of detectable compounds by IMS to include nonvolatile samples dissolved in a liquid solvent. More recently, an ultra-high resolution IMS system has been developed [6,7] and utilized successfully by our group to determine ion mobility constants of common amino acids in different drift-gases and to analyze amino acid mixtures [3]. The IMS technique has also been utilized successfully for analysis of biomolecular mixtures in an ESI/ion-trap/IMS/time-of-flight mass spectrometer for analysis of protein/peptide mixtures [8].

The fundamentals and applications of the IMS technique are reviewed in detail elsewhere [5]. In brief, ion mobility separates compounds on the basis of their gas-phase ion mobilities, commonly in N_2 or air, giving mobility constants (K^m) which are usually specified in units of $cm^2\,V^{-1}\,s^{-1}$, and defined as

$$K^m = \frac{\nu}{E} \tag{1}$$

where ν is the velocity of the ion and E is the electric field in the drift region of the spectrometer. Mobility constants are usually calculated by measuring the time an ion travels down the drift tube using a rearranged form of Eq. (1) given as

$$K^m = \frac{L^2}{Vt_\mathrm{d}} \tag{2}$$

Here, L is the ion drift distance, V is the voltage drop across L, and t_d is the time required for the ion to traverse L. The mobility of an ion depends on the neutral gas number density and temperature. The dependence on the number density is removed by reporting the ion mobility at temperature and pressure conditions corresponding to 273 K and 760 Torr, respectively. This reduced ion mobility is given by,

$$K_0^m = K^m \left(\frac{273}{T}\right)\left(\frac{P}{760}\right) \tag{3}$$

where T and P are the measured temperature and pressure, respectively.

Regardless of the resolving power of an instrument, it is clear that it is impossible to separate two compounds with identical K^m values. The use of different drift-gases alters the separation factor (α) in the IMS spectra and, thus, affects the separation selectivity [9]. The separation factor α is defined as

$$\alpha = \frac{K_0^1}{K_0^2} \tag{4}$$

where K_0^1 is the reduced mobility of the faster compound, and K_0^2 is that of the slower compound. Therefore, as in chromatography, a value of 1 indicates that two compounds cannot be separated with the current selectivity of the instrument.

It has recently been shown that α values in IMS can be changed by either operating in very high electric fields [10] or by using different drift-gas [3,9]. Asbury and Hill [9], and more recently Beegle et al. [3], have shown that changing the drift-gases composition (i.e., changing the polarizability of the drift-gas) can improve the ion mobility separation in IMS. By utilizing different drift-gases (namely He, Ar, N_2, and CO_2), Asbury and Hill [9] improved the separability of several low-weight compounds, including iodoaniline, chloroaniline, and three peptides. Beegle et al. [3] demonstrated that the separability of organic molecules (amino acids) can be greatly affected by the polarizability of the drift-gases employed (N_2, Ar, and CO_2). Utilizing different drift-gases effects, the drift time of a selected ion is calculated by means of the variation of the physical properties of the gas such as mass and collision cross-section [3,9]. This approach was theoretically investigated for first time over 25 years ago [11] and since then has been utilized in a number of investigations [12,13]. More recently, the use of helium as a drift-gas has found wide acceptance for measurements of collision cross-sections of biomolecules in the gas-phase due to the low polarizibility of He which avoids complications in theoretical calculations [14].

One of the primary goals in this investigation was to experimentally understand the processes that takes place in ion–molecule collisions in the IMS drift tube which can potentially lead to models of these complex interactions. It is hoped that such a model will enable a unique identification of molecules in a sample of unknown compounds.

2. Experimental apparatus

The ESI/IMS instrument used in this investigation was constructed at Washington State University (WSU) at Pullman. The details of the ESI unit have been given previously [15]. A detailed description and schematics of the high-resolution IMS instrument were also provided in an earlier publications [3,7,16]. In the next few paragraphs, we will briefly summarize the general operating conditions of the ESI/IMS apparatus.

The ion mobility spectrometer was interfaced to a CQ-150 quadrupole mass spectrometer (ABB Extrel, Pittsburgh, PA). The ions enter the mass spectrometer (MS) via a 40 μm aperture and were detected by an electron multiplier located at the back of the MS. The aperture served as the barrier between the atmospheric pressure of the IMS and the vacuum of the mass spectrometer. The ion mobility spectrometer had a drift length of 22.5 cm and was always operated in the positive mode using the following drift voltages: ∼6220 V for He and ∼7900 V for N_2, Ar, and CO_2, respectively.

The drift tube was held at a constant temperature of 250 °C and at local atmospheric pressure (∼700 Torr at Pullman, WA). A counter flow of preheated drift-gas (N_2, Ar, and CO_2) was introduced at the end of the drift region at a flow rate of ∼800 mL/min. Helium was introduced with a larger flow rate, ∼1400 mL/min, to reduce any effects of residual air molecules which might be present.

The sample solution was delivered via a liquid chromatography pump into a metal spray needle at a flow rate of 5 μL/min. The needle was air-cooled to prevent the heated drift/drying gas from causing solvent evaporation inside the needle. The electrospray was drawn by electric potential into the entrance of the desolvation region (7.2 cm in length) of the spectrometer, where the charged mist migrates in an electric field through a counter flow of heated drift-gas. During the few milliseconds of migration through the desolvation region, solvent evaporates from the droplets and ions are introduced into the drift region of the instrument through an ion gate located at the entrance. The gate is “open” for 0.2 ms and the ions are introduced into the drift region where they accelerate under the influence of an electric field. They then pass through a pinhole into the MS region and are detected

by the electron multiplier on the Extrel quadruple mass spectrometer.

All mobility data were collected by replacing the stock preamplifier with a Keithley 427 amplifier (Keithley Instruments, Cleveland, OH) and sending the amplified signal to the data acquisition system, again constructed at WSU. A detailed description of the IMS data control and acquisition system was reported previously [16]. All data taken were the average of 1000 individual 50 ms spectra resulting in a total experimental run time of less than 1 min.

All five compounds which were studied in this investigation, were purchased from Sigma Chemical Company (St. Louis, MO) and used without further purification. All solvents (water, acetic acid, and methanol) were HPLC grade and were purchased from J.T. Baker (Pillipsburgh, NJ). Samples were prepared by weighing out known quantities and then dissolving them in a solvent solution consisting of 47.5% water, 47.5% methanol, and 5% acetic acid. The sample concentrations used were approximately 5 ppm.

3. Results and discussion

Mobility spectra were obtained for each compound in each different drift-gas. The drift times were taken and both the mobilities, K^m, and the reduced mobilities, K_0^m, were calculated with the K_0^m values tabulated in Table 1. In all cases, the compounds drifted fastest in He followed by N_2, Ar, and CO_2, just as described elsewhere [9,13].

Ion–molecule collision cross-sections (Ω_m) were obtained using a rearranged form of the equation governing gas-phase ion transportation [11] shown as follows:

$$K^{-1} = \frac{16N}{3}\left(\frac{\mu kT}{2\pi}\right)^{1/2}\frac{\Omega_m}{q} \quad (5)$$

where N is the number density of the gas, μ is the reduced mass, k is the Boltzmann constant, T is the temperature in the drift region, q is the charge on the ion, and K is the mobility of the ion measured with ion mobility spectrometry. The ion–molecule collision cross-sections values Ω_m are tabulated in Table 2 for each compound in each drift-gas.

Table 2
Collision cross-sections, Ω_m, calculated using Eq. (5) for the five compounds studied in different drift-gases

Compound	Ω_m (Å^2)			
	He	Ar	N_2	CO_2
Glycine	46.6	95.8	98.9	147.6
Triglycine	68.7	114.6	120.6	156.3
Tetraglycine	88.6	126.2	133.2	167.7
Pentaglycine	99.3	142.4	145.2	176.5
Hexaglycine	112.1	148.6	157.4	186.5

3.1. Calculation of drift-gas radii

In addition to diffusive forces and the effect of an external electric field, the motion of ions in the IMS drift tube is also affected by the electrostatic interaction between the ion and the drift-gas molecules. The electron cloud surrounding the neutral gas molecule is polarized both by the external electric field and by the ion, thus inducing a dipole moment in the neutral molecule. This results in an electrostatic interaction

Table 1
Reduced mobilities, K_0^m, and molecular weights for the five compounds studied in different drift-gases

Compound	MW (amu)	K_0^m			
		He	Ar	N_2	CO_2
Glycine (Gly)	75.07	8.91	1.64	1.81	1.03
Triglycine (Gly–Gly–Gly)	189.2	5.44	1.23	1.36	0.87
Tetraglycine (Gly–Gly–Gly–Gly)	246.2	4.60	1.09	1.21	0.79
Pentaglycine (Gly–Gly–Gly–Gly–Gly)	303.3	4.10	0.96	1.10	0.74
Hexaglycine (Gly–Gly–Gly–Gly–Gly–Gly)	360.3	3.63	0.91	1.00	0.69

between the ion and the neutral drift-gas molecule which is called the charge-induced dipole effect. In this article, two simple models—the "Langevin" and the "hard-sphere" models were utilized to calculate the drift-gas radii. A brief discussion of the models is given below.

3.1.1. The Langevin model

The Langevin model assumes the interaction between the ion and neutral molecules is due solely to the long-range ion-induced dipole interaction. The interaction potential, V_{pol}, which falls off as $\sim q^2\alpha_P/2r_d^4$ at large r_d where r_d is the distance between the ion and the neutral molecule and α_p is the polarizability of the drift-gas. The cross-section, which is often referred as "the Langevin cross-section", σ_L, is then given by:

$$\sigma_L = \pi r_L^2 = \pi\sqrt{\frac{2\alpha_P q^2}{kT}} \tag{6}$$

where r_L is the Langevin radius, and other parameters were defined previously. Eq. (6) can be used to calculate the Langevin radius or "charge-induced dipole capture radius" of the neutral molecule in question. Table 3 tabulates the Langevin radii for the drift-gases used (He, Ar, N_2, and CO_2) in this investigation.

3.1.2. The hard-sphere model

A simple hard-sphere model is also utilized in order to estimate the radii of the neutral drift-gas molecules. The model is based on the viscosity of the gas and is given by

$$r_{\text{gas}}^2 = \frac{1}{4}\left(\frac{5}{16\pi^{1/2}}\right)\left(\frac{(MRT)^{1/2}}{N_A\eta}\right) \tag{7}$$

Table 3
Polarizability and calculated radii for each of the drift-gases utilized in this work

Drift-gas	MW (amu)	Polarizability (10^{-24} cm^3)	Calculated radius (Å)[a]	Calculated radius (Å)[b]
He	4	0.205	3.38	1.03
Ar	40	1.641	5.69	1.67
N_2	28	1.740	5.77	1.73
CO_2	44	2.911	6.57	2.02

[a] Calculated radius using the Langevin model at the operating temperature of the IMS cell (250 °C).
[b] Calculated radius using the hard-sphere model.

where r_{gas} is the radius of the neutral drift-gas molecule, M is the mass of that molecule, R is the gas constant, T is the temperature, N_A is Avogadro's constant, and η is the viscosity of the gas [17]. The calculated radii (using hard-sphere model), the polarizability and the molecular weight (MW) of each drift-gas are given in Table 3.

A comparison of the drift-gas radii obtained by two models shows that the Langevin radii are approximately 2.3 times larger than those obtained from hard-sphere model. The fact that the Langevin radii are too large indicates that there is a fair amount of charge delocalization taking place in the ion. Thus, the neutral radii should be somewhere between the hard-sphere and the Langevin radii.

3.1.3. Calculation of ion radii

Calculation of the radii of the ions were approximated by utilizing the hard-sphere model. Unlike the Langevin model, this assumes that there is no long-range ion-induced dipole interaction between the ion and neutral drift-gas molecules. The model also assumes that the ions are influenced by the electric field. However, as mentioned above, because of the combined effects of long-range ion-molecule interaction and the external electric field, the drift-gas molecules do become polarized and, hence their radii changes.

Under the assumptions of the hard-sphere model, the collision cross-section is reduced to $\Omega_m = \pi(r_{\text{ion}} + r_{\text{gas}})^2$ where r_{ion} is the radii of the ions. The assumption that the ions in consideration here (glycine peptides) are nearly spherical is supported by previous molecular modeling and ion mobility studies on oligoglycines (Gly_n, $n = 1$–6) [18]. These ion mobility studies approximated average equilibrium geometries of these ions which were found to be nearly spherical. Therefore, the radii of the ions were calculated by using the following formula,

$$r_{\text{ion}} = \left(\frac{\Omega_m}{\pi}\right)^{1/2} - r_{\text{gas}} \tag{8}$$

Since the collision cross-section is a measured quantity (see Eq. (5)), any systematic error in r_{gas} will directly effect the r_{ion} calculation.

It should be noted that the long-range ion-molecule interactions became more important when the polarizability of the drift-gas increases. Long-range ion-molecule interactions decrease ion mobility and, thus, increase measured ionic size according to the following relation:

$$\Omega_{\mathrm{m}} = \Omega_P + \Omega_{\mathrm{a}} \tag{9}$$

where Ω_{m} is the collision cross-section measured with ion mobility spectrometry (see Eq. (5)), Ω_p is the contribution to the measured collision cross-section due to the polarizability of the ion molecule interaction, and Ω_{a} is the actual ion–molecule collision cross-section. For the purpose of this discussion, as mentioned above, ion size was determined using the hard-sphere model in which $\Omega_{\mathrm{m}} = \pi(r_{\mathrm{eff}} + r_{\mathrm{gas}})^2$ and, thus,

$$r_{\mathrm{eff}} = r_{\mathrm{pol}} + r_{\mathrm{act}} \tag{10}$$

where r_{eff} is the experimentally obtained "*effective*" ion radius, r_{pol} is that portion of the radius which is due to the ion–molecule long-range polarization interaction, and r_{act} is the actual ion radius. This implies that the experimentally obtained "effective" ion radius, r_{eff}, should increase with the increasing polarizability of the drift-gas. In fact, this picture is consistent with our results. In He, the radius of the ion is smaller than in Ar or N_2, and in CO_2 it is significantly larger (by about 75% than in He as seen from Table 4). Obviously, one of the degrees to which the hard-sphere model is no longer adequate in describing the situation is directly related to the polarizability of the drift-gas used.

Table 4
Calculated ion radius for each of the compounds in different drift-gases

Compound	MW (amu)	Ion radius (Å)			
		He	Ar	N_2	CO_2
Glycine	75.07	2.82	3.84	3.88	4.84
Triglycine	189.2	3.65	4.37	4.47	5.03
Tetraglycine	246.2	4.28	4.67	4.78	5.29
Pentaglycine	303.3	4.59	5.06	5.07	5.48
Hexaglycine	360.3	4.94	5.21	5.35	5.69

As mentioned earlier, once the K_0^m values were determined it was possible to calculate the collision cross-section (Ω_{m}) for each ion using Eq. (5). Radii were then calculated for each of the five compounds and are tabulated in Table 4. As was the case previously ([9], referred to henceforth as Asbury) the calculated radius changes depending on the drift-gas used. The calculated radius increased in the same relation as was previously reported (from He to Ar to N_2 to CO_2). Since the ions were mass selected (only protonated molecules were allowed to pass) via the quadrupole mass filter, it is believed that the ions produced were the same in each drift-gas and, thus, does not account for the differences in calculated radii. Amino acids generally have the same K_0^m values for drift temperatures between 180 and 250 °C in both N_2 and CO_2 [3,9], respectively, suggesting that clustering is not taking place inside of the drift tube.

Asbury, based on his empirical observation, showed that a linear relationship exists between the ion radii and the polarizability of the drift-gas for the limited number of drift-gases they used in their investigation. Using the same approach, we plotted the calculated ion radius (see Table 4) versus drift-gas polarizability (see Table 3) for each compound as shown in Fig. 1. The linear regression data for each line are tabulated in Table 5. Table 5 also provides R^2 values. The R^2 values for all the compounds studied here (with the exception of hexaglycine) are found to be greater than 0.99 indicating that a linear relationship exists between the calculated radius and the drift-gas polarizability. However, it should be noted here that, in general, a linear relationship between the radius of ion and the drift-gas polarizability should not be expected.

Table 5
Regression data for each of the curves shown in Fig. 1

Compound	Charge	Slope	Intercept	R^2
Glycine	1	0.744	2.6	0.997
Triglycine	1	0.511	3.6	0.999
Tetraglycine	1	0.370	4.1	0.992
Pentaglycine	1	0.328	4.5	0.999
Hexaglycine	1	0.276	4.9	0.961

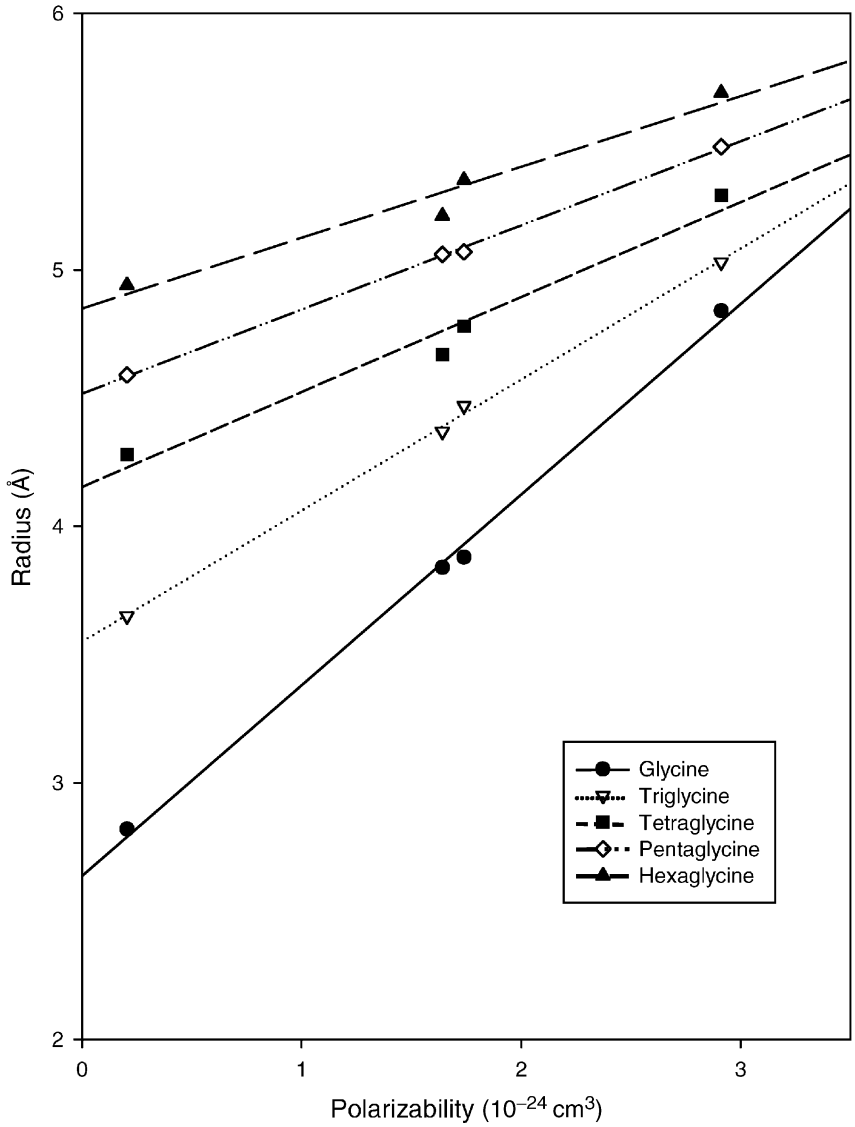

Fig. 1. Radius vs. polarizability for the five compounds studied. The drift-gases used were He (polarizibility of 0.205×10^{-24} cm^3), Ar (1.641×10^{-24} cm^3), N_2, (1.740×10^{-24} cm^3), and CO_2 (2.911×10^{-24} cm^3).

This relationship should hold only in a limited range of polarizabilities (where the long-range ion-induced dipole interaction between the ion and neutral drift-gas molecules is weak) and where the cross-sections of both the neutral gas molecule and the ion are dictated by their geometry, which will be discussed later. It can be clearly seen in Fig. 1 that the ion radii measured in He are nearly identical with the intercepts indicating that helium is nearly a hard-sphere and that the cross-sections for the ions measured in helium are dominated by the geometry of the ion and not the long-range dipole interaction between helium atoms and the ions. The dipole interaction is weak due to the small polarizability value of He (0.205×10^{-24} cm^3).

One can express the linear relationship between the effective ion radii and polarizability of the drift-gases in the following manner:

$$r_{\text{eff}} = m\alpha_p + r_{\text{act}} \quad (11)$$

where m is the slope of the line and α_p is the polarizability of the drift-gas. If we interpret that slope as a measure of charge density on the ion, then a smaller molecule will have a greater charge density than a larger one and, hence, more interaction with the drift-gas due to drift-gas polarizability takes place. As seen in Fig. 1, the slopes decrease with increasing ion size indicating that the ion–molecule interaction is less an issue as the size of the ions increase as expected. This is because, for larger ions, the cross-section is determined mostly by the geometry of the ion while for smaller ions, the secondary effect on the measured cross-section (or radius) of an ion, due to long-range interaction with the drift-gas, becomes more important.

The slope of the line provides information on the magnitude of the ion's mobility change with polarizability whereas the intercept provided the gas-phase radius of the ion in a "hypothetical" unpolarizable medium. The plots show that the slope changed by approximately 2.7 times, from 0.744 for glycine to 0.276 for hexaglycine, while the *y*-intercept values, which represent the radius of the ions in a non-polarizing gas (and hence the actual ion radius, r_{act}) increased by ~0.4 Å as each additional glycine is added to the peptide chain.

A "breakdown" in the linear relationship between the ion radii and drift-gas polarizability occurs when the polarizability of the drift-gas exceeds a certain limit at which the cross-section (or radius) of the ions are determined not only by their geometry but also from long-range dipole interaction between the drift-gas molecules and ions. To test the limit where this breakdown occurs, we calculated the ion radii from the reduced mobility constants of the nine aliphatic amines and eight aromatic amines reported by Karpas and Berant [13] (referred to henceforth as Karpas) where the ion mobility constants were measured in He, Ar, CO_2, and SF_6, in addition to N_2 added for the aliphatic amines. Figs. 2 and 3 shows the radius versus polarizability for four of the data points reported in Karpas (two aliphatic amines and two aromatic amines). As was the case for both the present work and Asbury, Karpas's radius versus polarizability data, when plotted for He, N_2, Ar, and CO_2, exhibit a linear relationship (see Fig. 2). However the relationship fails when a high-polarizability gas, such as SF_6 (which has a polarizability of 6.54×10^{-24} cm^3), is included (see Fig. 3). As previously discussed, this breakdown can be attributed to the "simple" hard-sphere model in which the effects of the long range ion–molecule interactions is not taken into account. This is evident in Tables 6 and 7 where regressions for the Karpas data are shown both for aromatic amines and aliphatic amines, respectively. When the

Table 6
Comparison of the linearity of the ion radius vs. drift gas polarizibility in aliphatic amines with and without SF_6.

Compound	Ion mass/MW	With SF_6		Without SF_6	
		Slope	R^2	Slope	R^2
Ethylamine	46	0.3931	0.8050	0.8371	0.9869
n-Propylamine	60	0.3509	0.8251	0.7067	0.9549
Trimethylamine	60	0.3076	0.8141	0.6392	0.9688
n-Butylamine	74	0.3466	0.8064	0.7041	0.9179
Triethylamine	102	0.2296	0.8585	0.4253	0.9434
Di-*n*-butylamine	130	0.1915	0.8288	0.3602	0.8849
Tributylamine	186	0.1342	0.8288	0.2085	0.9033
Tri-*n*-octylamine	354	0.4751	0.9111	0.5840	0.9606
Tridodecylamine	522	0.7225	0.9818	0.0726	0.5778

Table 7
Comparison of the linearity of the ion radius vs. drift gas polarizibility in aromatic amines with and without SF_6.

Compound	Ion mass/MW	With SF_6		Without SF_6	
		Slope	R^2	Slope	R^2
Pyridine	80	0.323	0.8424	0.8503	0.9995
4-Picoline	94	0.2847	0.8480	0.7157	0.9767
Aniline	94	0.2777	0.8535	0.6512	0.9964
2,4-Lutidine	108	0.2555	0.8807	0.7122	0.9631
2,4,6-Collidine	122	0.2200	0.8785	0.5947	0.9709
2-Ethylanine	122	0.2277	0.8474	0.4417	0.9628
Quinoline	130	0.2498	0.8746	0.3709	0.9829
2-Isopropylanine	136	0.2278	0.8573	0.2227	0.9291

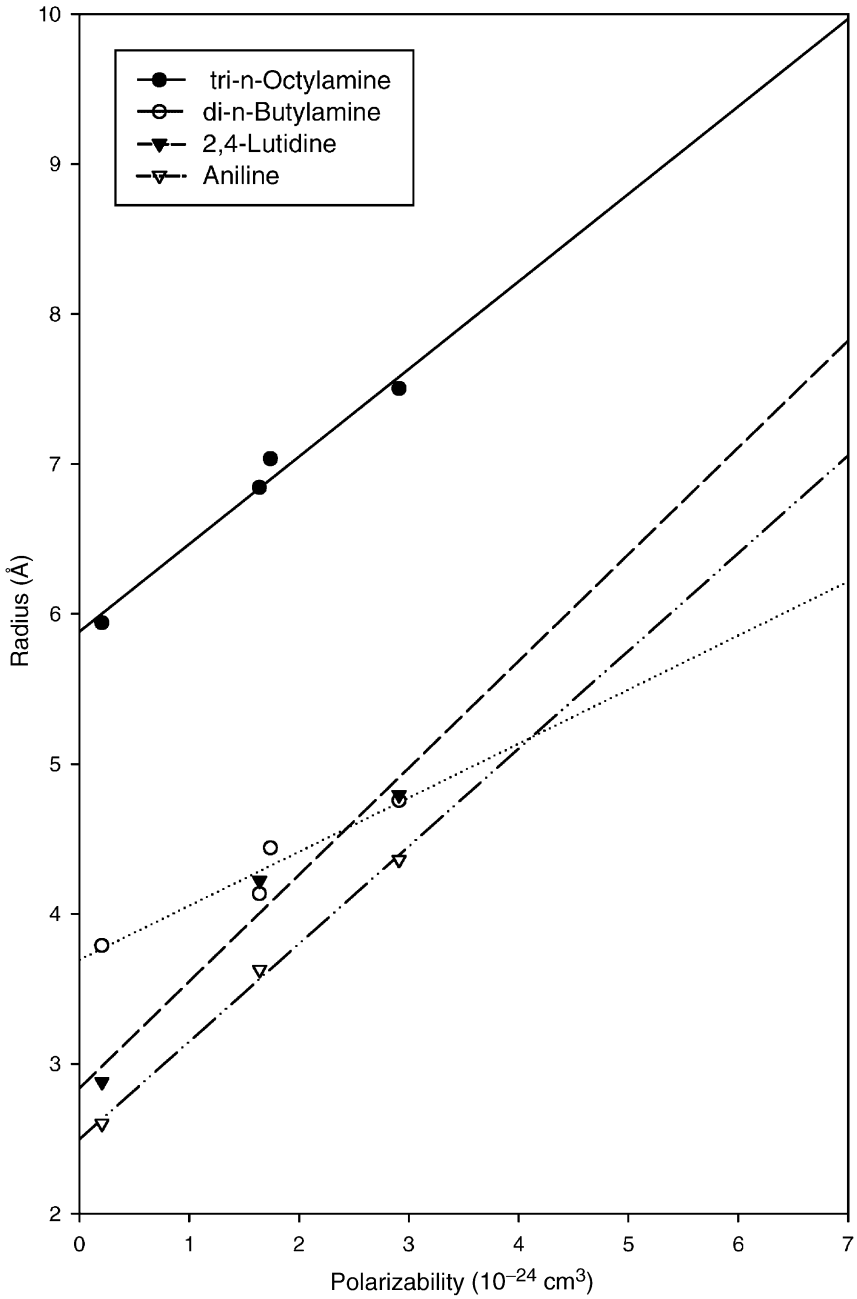

Fig. 2. Radius vs. polarizability for four compounds found in Karpas and Berant [13] without the data point representing SF_6. The circles represent aliphatic amines and the triangles are aromatic amines. The drift-gases used were He (polarizibility of 0.205×10^{-24} cm^3), Ar (1.641×10^{-24} cm^3), N_2, (1.740×10^{-24} cm^3), and CO_2 (2.911×10^{-24} cm^3).

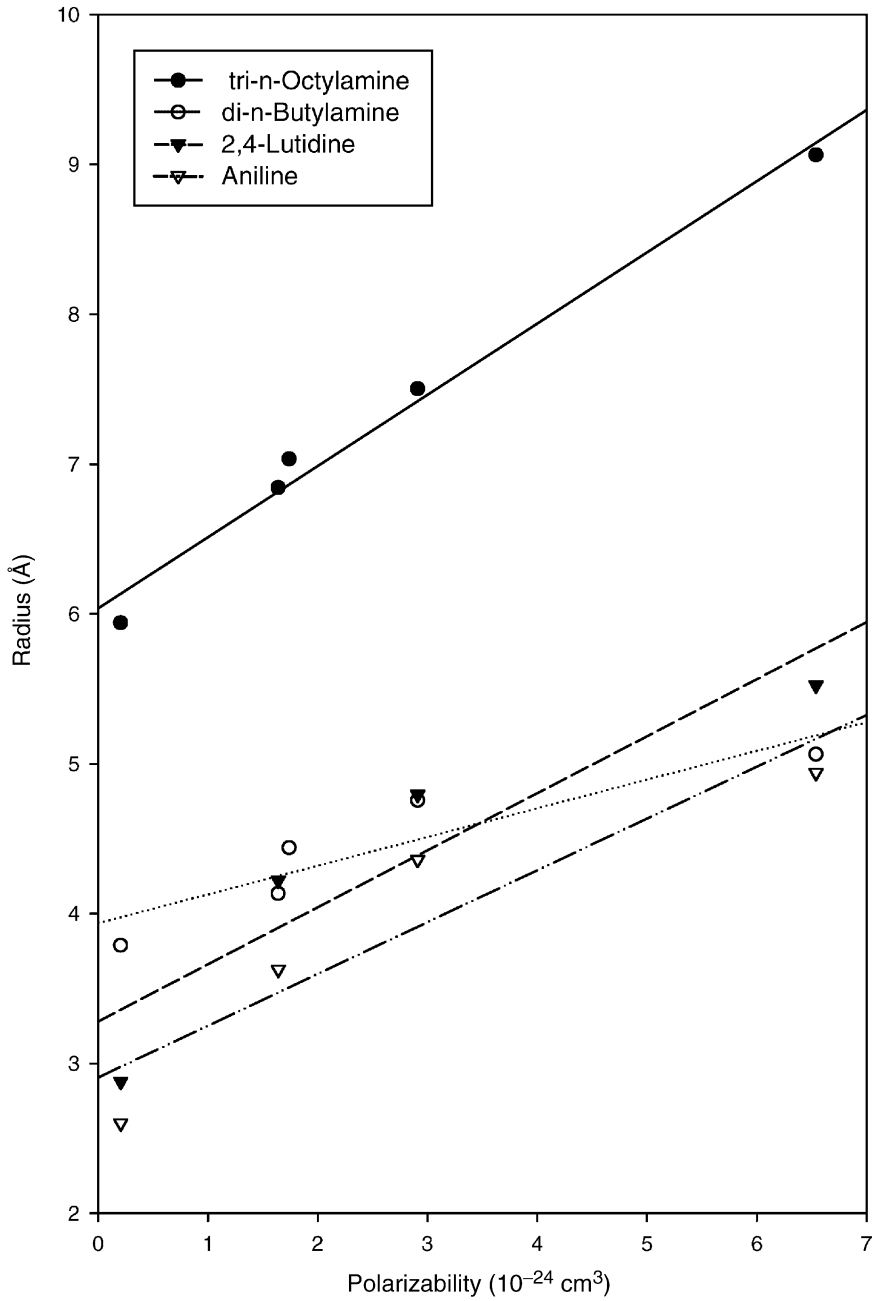

Fig. 3. Radius vs. polarizability for four compounds found in Karpas and Berant [13]. When the data points representing the SF_6 are included the linear relationship breaks down. The circles represent aliphatic amines and the triangles are aromatic amines. The drift-gases used were He (polarizibility of 0.205×10^{-24} cm^3), Ar (1.641×10^{-24} cm^3), N_2, (1.740×10^{-24} cm^3), CO_2 (2.911×10^{-24} cm^3), and SF_6 (6.54×10^{-24} cm^3).

highly polarizable drift-gas SF_6 was used, the effects due to long-range ion-molecule interactions become much more important. Finally, the linear relationship between the radius of an ion and the polarizability of a drift-gas also depends on the geometric shape of the molecular ion under investigation as suggested by the Karpas data, where the aliphatic amines exhibited a much stronger linearity with respect to polarizability than did the aromatic amines when the just lighter drift-gases (He, Ar, N_2, and CO_2) were taken into consideration (see Tables 6 and 7).

4. Summary and conclusions

In this work, we report the ion mobility constants of glycine along with four peptide compounds (triglycine, tetraglycine, pentaglycine, and hexaglycine) in four different drift-gases (He, Ar, N_2, and CO_2). We also report the effects of different drift-gases in IMS on the calculated ion radii of the peptide compounds. In this present investigation, it was found that that the ion charge distribution, which is influenced by the external electric field and long-range ion molecule interaction, can affect the collision process and thus the measured ion mobilities. This can result in the change of arrival order of two different ions in different drift-gases. We empirically observed that a linear relationship exists between the ion radius and polarizability of the drift-gas used when the drift-gas is not highly polarizable. Our data, as well as others (Asbury and Karpas) show that polarizability does not affect all ions equally. In fact, Asbury demonstrated that compounds can have different arrival sequences under different drift-gases. For example, the compounds chloroaniline drifts faster then iodaniline in He, while in CO_2 the reverse is true. The source of this phenomenon is currently being explored in our laboratory. Clustering effects between ion and gas molecules inside the drift tube are considered to be negligible due to the fact that the reduced mobilities of the ions are independent of temperature at the elevated temperatures (250 °C) under which we are operating.

We acknowledge that both the Langevin model and the hard-sphere model represent only an approximation to the real physical processes that take place inside the drift tube. Therefore, a new model is being developed which takes into account not only the polarizability of both the drift-gas and the ion, but also local electric fields inside the drift region.

Polarizability effects change the calculated ion radii in a linear fashion but does not affect all the ions equally. This can be utilized to change the separation factor in IMS since all ions that yield different slopes can theoretically be separated using different drift-gases. However as the polarizability of the drift-gas is increased, the linear relationship breaks down. Therefore, it appears that it would be possible to exploit the polarizability effect to increase separation between target ions if one utilized drift-gases in which the linear relationship holds. The present data shows that when a judicial choice of drift-gas is made, a much improved separation of target ions can be achieved. Our work indicated that He and CO_2 are two good candidate drift-gases for this purpose.

Acknowledgements

The research described in this paper was carried out at the Jet Propulsion Laboratory, California Institute of Technology, and at the Washington State University at Pullman, WA and sponsored by the National Aeronautics and Space Administration's Planetary Instrument Definition and Development Program Office, and the Jet Propulsion Laboratory, Director's Discretionary Fund (Grand Challenge). We appreciate the critical reading of Dr. Paul V. Johnson. We greatly appreciate the comments of two anonymous referees for improving the work described here.

References

[1] P.J. Boston, M.V. Ivanov, C.P. McKay, Icarus 95 (1992) 300.
[2] J.D. Anderson, E.L. Lau, W.L. Sjogren, G. Schubert, W.B. Moore, Science 276 (1997) 1236.
[3] L.W. Beegle, I. Kanik, L. Matz, H.H. Hill, Anal. Chem. 73 (2001) 3082.

[4] H.H. Hill, W.F. Siems, R.H. St. Louis, D.G. McMinn, Anal. Chem. 62 (1990) A1201.
[5] G.A. Eiceman, Z. Karpas, Ion Mobility Spectrometry, CRC Press, Boca Raton, Fl, 1994.
[6] G.R. Asbury, Ph.D. Thesis, Washington State University, 1999.
[7] G.R. Asbury, H.H. Hill, J. Microcolumn. 3 (2000) 172.
[8] S.C. Henderson, S.J. Valentine, A.E. Couinterman, D.E. Clemmer, Anal. Chem. 71 (1999) 291.
[9] G.R. Asbury, H.H. Hill, Anal. Chem. 72 (2000) 580.
[10] R.W. Purvis, R. Guevremont, Anal. Chem. 71 (1999) 2346.
[11] H.E. Revercomb, E.A. Mason, Anal. Chem. 47 (1975) 970.
[12] H.W. Ellis, R.Y. Pai, I.R. Gatland, E.W. McDaniel, R. Wernlund, M.J. Cohen, J. Chem. Phys. 64 (1976) 3935;
E.S. Sennhauser, D.A. Armstrong, Can. J. Chem. 56 (1978) 2337;
T.W. Carr, Anal. Chem. 51 (1979) 705;
E.S. Sennhauser, D.A. Armstrong, Can. J. Chem. 58 (1980) 231;
Z. Berant, Z. Karpas, O.J. Shahal, Phys. Chem. 93 (1989) 7529;
T. Yamashita, et al., Nucl. Instrum. Methods Phys. Res. A283 (1989) 709;
M.D. Perkins, R.D. Chelf, F.L. Eisele, E.W. McDaniel, J. Chem. Phys. 79 (1983) 5207.
[13] Z. Karpas, Z. Berant, Phys. Chem. 93 (1989) 3021.
[14] G. von Helden, T. Wyttenbach, M.T. Bowers, Science 267 (1995) 1483;
D.E. Clemmer, R.R. Hudgins, M.F. Jarrold, J. Am. Chem. Soc. 117 (1995) 10141;
S.J. Valentine, J.G. Anderson, A.D. Ellington, D.E. Clemmer, J. Phys. Chem. B 101 (1997) 3891;
S.J. Valentine, A.E. Cointerman, D.E. Clemmer, J. Am. Soc. Mass Spectrom. 8 (1997) 954.
[15] D. Wittmer, Y.H. Chen, B.K. Luckenbill, H.H. Hill, Anal. Chem. 66 (1994) 2348.
[16] C. Wu, W.F. Siems, G.R. Asbury, H.H. Hill, Anal. Chem. 70 (1998) 4929.
[17] D.R. Lide (Ed.), CRC Handbook of Chemistry and Physics, eightieth ed., CRC Press, Boca Raton, Fl, 2000.
[18] T. Wyttenbach, J.E. Bushnell, M.T. Bowers, J. Am. Chem. Soc. 120 (1998) 5098.